10th ANKARA INTERNATIONAL AEROSPACE CONFERENCE **AIAC-2019-077**
18-20 September 2019 - METU, Ankara TURKEY

# VIBRATION ANALYSIS OF AXIALLY FUNCTIONALLY GRADED ROTOR BLADES

Burak Kilic[1] and Ozge Ozdemir[2]
Istanbul Technical University
Istanbul, Turkey

## ABSTRACT

*Functionally Graded Materials (FGMs) are special composites that have continuous variation of material properties in one or more directions to provide designers with the ability to distribute strength and stiffness in a desired manner to get suitable structures for specific purposes in engineering and scientific fields. As a consequence, it is important to understand the static and dynamic behavior of FGMs so it has been an area of intense research in recent years.*
*In this study, a MATLAB code has been developed to examine the free vibration behavior of rotor blades modeled as axially functionally graded rotating Timoshenko and Euler – Bernoulli beams.*

## INTRODUCTION

The first application for functional graded materials (FGM) was carried out in 1984 in an aviation and space project in Japan. In the mentioned study, a thermal barrier with a temperature of 2000 K on one surface and a temperature resistance of 1000 K on the other surface and a gradient of temperature resistance across the structure and a cross-section of less than 10 mm was developed [Chen and Liew, 2004].

In their study, Huang and Li studied the free vibrations of axially functional graded beams with a non-uniform cross section. In order to find the natural frequencies of the beams with varying bending rigidity and variable density, the conservation equation with various coefficients was converted to the Fredholm integral equation to obtain natural frequency results [Huang and Li, 2010].

Alshorbagy, Eltaher and Mahmod have studied the free vibrations of functionally graded beams by using finite element method. The equations of motion of the beam are developed using the classical Euler-Bernoulli beam theory and the virtual business principle. In the study, the cases where the beam material properties vary both in thickness and in the axial direction, were investigated separately. In addition, the effects of different beam boundary conditions, the degree of gradient formula and the fineness ratio of the beam on the natural frequencies were investigated [Alshorbagy, Amal, Eltaher and Mahmoud, 2011].

In 2011, Shahba et al. developed a solution using the finite element method to determine the free vibration of the axially functional graded beams. Within the scope of the study, proper

[1] Master Student in Aeronautics Engineering, Email: kilicburak@itu.edu.tr
[2] Assoc. Prof. in Aeronautics Engineering , Email: ozdemirozg@itu.edu.tr

shape functions were determined for Timoshenko beam, and an equation was created to express the material and contraction changes along the beam. After formation of the formulation, free material equation factors and free vibration under boundary conditions were examined. Then, the effect of different contraction factors on the free vibration values was investigated [Shahba et al., 2011].

In 2013, Rajasekaran studied the free vibration of the axially functional graded Euler - Bernoulli beams with different boundary conditions. In the study, the results were compared using both the Differential Transformation Method (DTM) and the lowest-order differential quadrature element method (DQEL). In order to examine the adequacy of these two methods within the scope of the study, non-homogeneous material status, taper ratio, rotational speed, rotor core radius and end mass were obtained according to the criteria such as the results and comparisons were made [Rajasekaran and Sundaramoorthy, 2013].

## METHOD

### Functionally Graded Beam Model

In this study, free vibration analysis of a rotating axially functionally graded (AFG) Timoshenko beam model, whose material properties vary in the axial direction, with a right-handed Cartesian coordinate system which is represented by Fig. 1., is carried out.

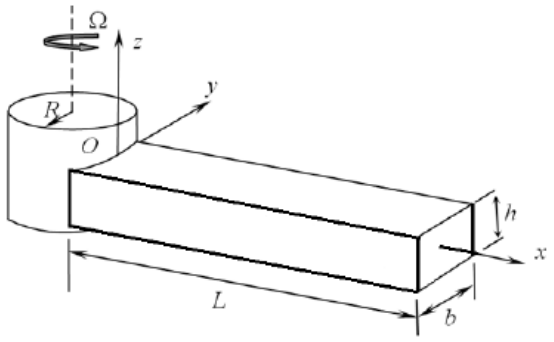


Figure 1. Rotating, Axially Functionally Graded Beam Model

Here, a rotating, axially functionally graded beam of length L, which is fixed at point O to a rigid hub with radius $R$, is shown. The beam height is h and width is b with cantilever boundary condition at point O is shown. The $xyz$ axes represent a global orthogonal coordinate system with its origin at the root of the beam. The beam is assumed to be rotating in the counter-clockwise direction at a constant angular velocity, Ω. In the right-handed Cartesian coordinate system, the $x$ -axis coincides with the neutral axis of the beam in the undeflected position, the $z$-axis is parallel to the axis of rotation, but not coincident and the $y$-axis lies in the plane of rotation.

#### Axially Functionally Graded Beam

Material properties of the beam, i.e. modulus of elasticity E, shear modulus G, Poisson's ratio $\nu$ and material density ρ are assumed to vary continuously in the axial direction, x, as a function of the volume fraction and the properties of the the constituent materials according to a simple power law.

According to the rule of mixture, effective material property T(x) can be expressed as follows:

$$T(x)=(T_R-T_L)\left(\frac{x}{L}\right)^n+T_L \quad n\geq 0 \tag{1}$$

where $T_L$ and $T_R$ are the material properties at the left and right ends of the beam, respectively and n, is a non-negative power law index parameter that dictates the material variation profile along the beam axis.

$$\rho(x)=(\rho_R-\rho_L)\left(\frac{x}{L}\right)^n+\rho_L \tag{2}$$

$$E(x)=(E_R-E_L)\left(\frac{x}{L}\right)^n+E_L \tag{3}$$

$$\upsilon(x)=(\upsilon_R-\upsilon_L)\left(\frac{x}{L}\right)^n+\upsilon_L \tag{4}$$

Energy Expressions for Euler Bernoulli Beam Model

In this section, derivation of the potential and kinetic energy expressions of a rotating Euler-Bernoulli Beam are carried out in great detail by using several explanatory figures and tables.

The cross-sectional and the longitudinal views of an Euler-Bernoulli beam that undergoes flapwise bending deflection are given in Fig. 2 and Fig.3, respectively. Here, the reference point is chosen, and is represented by $P_0$ before deformation and by P after deformation (Ozdemir Ozgumus, 2012).

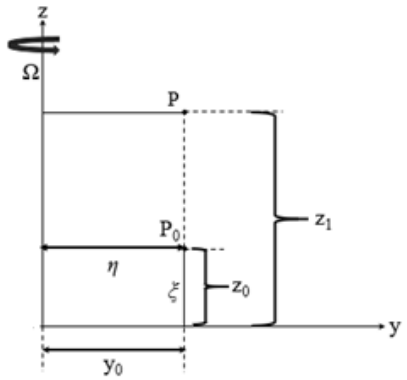


Figure 2. Cross-sectional View of the Euler – Bernoulli Beam

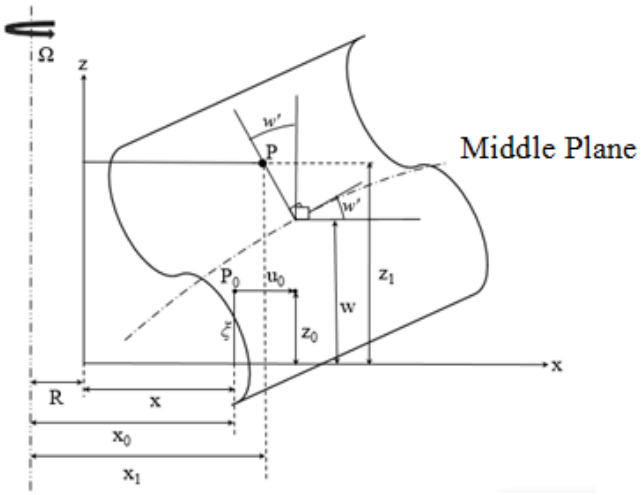


Figure 3. Longitudinal View of the Euler – Bernoulli Beam

Here; y and z are the global coordinates while η and ξ are the corresponding local coordinates. Coordinates of the reference point, $P_0$ before deformation are given as follows.

$$x_0 = R + x \tag{5}$$

$$y_0 = \eta \tag{6}$$

$$z_0 = \xi \tag{7}$$

Coordinates of the reference point, P after deformation are given as follows.

$$x_1 = R + x + u_0 - \xi w' \tag{8}$$

$$y_1 = \eta \tag{9}$$

$$z_1 = w + \xi \tag{10}$$

Strain field has to be defined for the reference point to be able to derive the kinetic and potential energy expressions. Therefore, the strain tensor $[\varepsilon_{ij}]$ is obtained as follows.

$$d\vec{r}_1.d\vec{r}_1 - d\vec{r}_0.d\vec{r}_0 = 2\begin{bmatrix} dx & d\eta & d\xi \end{bmatrix}\begin{bmatrix} \varepsilon_{ij} \end{bmatrix}\begin{Bmatrix} dx \\ d\eta \\ d\xi \end{Bmatrix} \tag{11}$$

The position vectors of the reference point are represented by $r_0$ and $r_1$ before and after deflection, respectively. Therefore, $dr_0$ and $dr_1$ can be written as follows.

$$d\vec{r}_0 = dx\vec{i} + dy\vec{j} + dz\vec{k} \tag{12}$$

$$d\vec{r}_1 = (1 + u_0' - \xi w'')\vec{i} + d\eta\vec{j} + (w'dx + d\xi)\vec{k} \tag{13}$$

where $(\cdot)'$ denotes differentiation with respect to the spanwise coordinate x.
Here, the strain tensor is

$$\left[\varepsilon_{ij}\right]=\begin{bmatrix}\varepsilon_{xx} & \varepsilon_{x\eta} & \varepsilon_{x\xi}\\ \varepsilon_{\eta x} & \varepsilon_{\eta\eta} & \varepsilon_{\eta\xi}\\ \varepsilon_{\xi x} & \varepsilon_{\xi\eta} & \varepsilon_{\xi\xi}\end{bmatrix} \tag{14}$$

Substituting Eqn. (12) and Eqn.(13) into Eqn. (11), the components of the strain tensor are obtained as follows

$$\varepsilon_{xx}=u_0'-\xi w''+\frac{(u_0')^2}{2}+\frac{\xi^2(w'')^2}{2}-u_0\theta'\xi \tag{15}$$

$$\varepsilon_{x\eta}=0 \tag{16}$$

$$\varepsilon_{x\xi}=\xi w'w''-u_0'w' \tag{17}$$

In this work, only $\varepsilon_{xx}$, $\gamma_{x\xi}$ and $\gamma_{x\eta}$ are used in the calculations because for long slender beams, the axial strain $\varepsilon_{xx}$ is dominant over the transverse normal strains $\varepsilon_{\eta\eta}$ and $\varepsilon_{\xi\xi}$ Moreover, the shear strain $\gamma_{\xi\eta}$ is by two orders smaller than the other shear strains $\gamma_{x\xi}$ and $\gamma_{x\eta}$. Therefore, $\varepsilon_{\eta\eta}$, $\varepsilon_{\xi\xi}$ and $\gamma_{\xi\eta}$ are neglected [Hodges and Dowell, 1974].
In order to obtain simpler expressions for the strain components given by Eqns. (15)-(17), higher order terms can be neglected, so an order of magnitude analysis is performed by using the ordering scheme taken from (Hodges and Dowell, 1974) and introduced in Table 1.

Table 1: Ordering Scheme for An Euler Bernoulli Beam

| | |
|---|---|
| $\frac{x}{L}=O(1)$ | $\frac{w}{L}=O(\varepsilon)$ |
| $\frac{\eta}{L}=O(\varepsilon)$ | $\frac{\xi}{L}=O(\varepsilon)$ |
| $\frac{u_0}{L}=O(\varepsilon^2)$ | |

Applying the ordering scheme to Eqns. (15)-(17), the simplified strain components are obtained.

Derivation of the Potential Energy Expression

The general expression for the potential energy is given by

$$U=\frac{1}{2}\int_0^L\left(\iint_A E\varepsilon_{xx}{}^2\,d\eta d\xi\right)dx \tag{18}$$

The area integrals given by (Hodges and Dowell, 1974), i.e. Table 2, are used in the derivation of the potential energy expressions.

Table 2: Area Integrals for Potential Energy Derivation

| | | |
|---|---|---|
| $\iint_A d\eta d\xi = A$ | $\iint_A \xi^2 d\eta d\xi = I_y$ | $\iint_A \eta^2 d\eta d\xi = I_z$ |
| $\iint_A (\eta^2 + \xi^2) d\eta d\xi = J$ | | $\iint_A \xi\eta d\eta d\xi = I_{yz} = 0$ |

Substituting the simplified strain field components into Eqn.(18) and applying the area integrals given by Table 2, the final expression for the potential energy is obtained.

The uniform strain $\varepsilon_0$ and the associated axial displacement $u_0$ due to the centrifugal force $F_{CF}(x)$ is given by

$$u_0' = \varepsilon_0(x) = \frac{F_{CF}(x)}{EA} \tag{19}$$

where EA is the axial stiffness, A is the cross-sectional area of the beam and the centrifugal force is

$$F_{CF}(x) = \int_x^L \rho A \Omega^2 (R + x) dx \tag{20}$$

Here; Ω is the rotational speed.

Substituting Eqn. (19) and Eqn. (20) into Eqn. (18) gives the final form of the potential energy as follows

$$U = \frac{1}{2}\left[EI_y(\theta')^2 + F_{CF}(x)(w')^2\right]dx + C_1 \tag{21}$$

where $I_y$ is the moment of inertia about the y-axis, w is the out-of-plane (flapwise) bending displacement and $C_1$ is the integration constant.

Derivation of the Kinetic Energy Expression

The general expression for the kinetic energy is given by

$$T = \frac{1}{2}\int_0^L \left( \iint_A \rho(V_x^{\,2} + V_x^{\,2} + V_x^{\,2}) d\eta d\xi \right) dx \tag{22}$$

For a rotating system, the velocity field is defined as follows (Ozdemir, 2019).

$$\vec{V} = \frac{\partial \vec{r_1}}{\partial t} + \Omega \vec{k} \, x \, \vec{r_1} \tag{23}$$

Considering the coordinate components given by Eqns. (8)-(10), the location vector $\overrightarrow{r_1}$ is substituted into Eqn.(23) and the velocity components are obtained.

The area integrals given by (Ozgumus Ozdemir and Kaya, 2008), i.e. Table 3, are used in the derivation of the kinetic energy expressions.

Table 3. Area Integrals for Kinetic Energy Derivation

| | |
|---|---|
| $\iint_A \rho d\eta d\xi = m$ | $\iint_A \rho \eta^2 d\eta d\xi = \rho I_z$ |
| $\iint_A \rho \xi d\eta d\xi = 0$ | $\iint_A \rho \xi^2 d\eta d\xi = \rho I_y$ |

Substituting the obtained velocity components into Eqn.(22) and applying the area integrals given by Table 3, the final expression for the kinetic energy is obtained

$$T = \frac{1}{2}\int_0^L (\rho A \dot{w}^2 + \rho I_y \dot{w}'^2 + \rho I_y \Omega^2 w'^2) dx + C_2 \tag{24}$$

where $C_2$ is the integration constant.

Timoshenko Beam Model

In this section, derivation of the potential and kinetic energy expressions of a rotating Timoshenko Beam are carried out in great detail by using several explanatory figures and tables.

The cross-sectional and the longitudinal views of a Timoshenko beam that undergoes flapwise bending deflection are given in Fig.4 and Fig.5, respectively. Here, the reference point is chosen and is represented by $P_0$ before deformation and by P after deformation (Ozdemir, 2019).

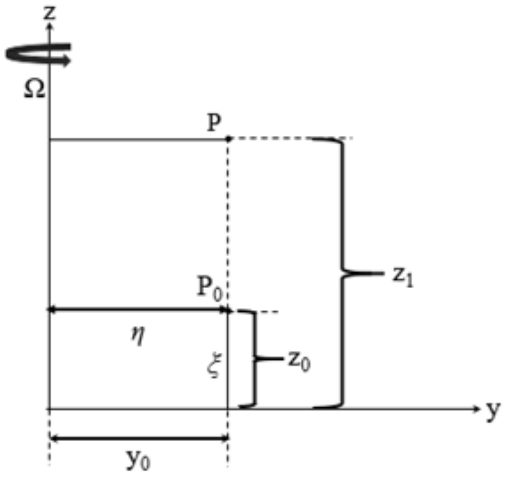


Figure 4: Cross-sectional View of the Timoshenko Beam

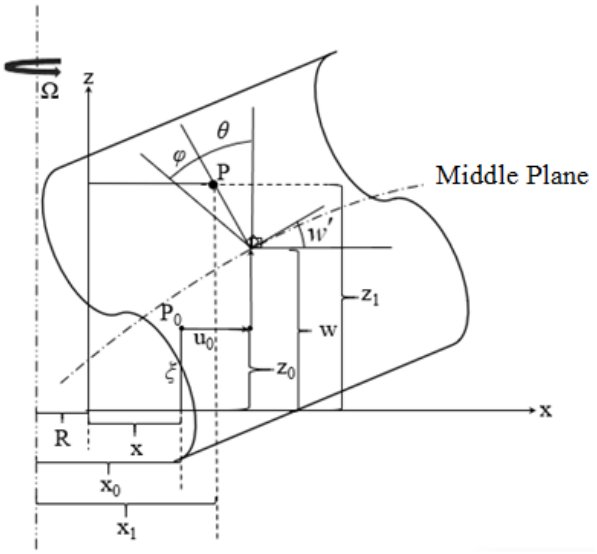


Figure 5: Longitudinal View of the Timoshenko Beam

Coordinates of the reference point, $P_0$ before deformation are given as follows.

$$x_0 = R + x \tag{25}$$

$$y_0 = \eta \tag{26}$$

$$z_0 = \xi \tag{27}$$

Coordinates of the reference point, $P_1$ after deformation are given as follows.

$$x_1 = R + x + u_0 - \xi\theta \tag{28}$$

$$y_1 = \eta \tag{29}$$

$$z_1 = w + \xi \tag{30}$$

The position vectors of the reference point are represented by $r_0$ and $r_1$ before and after deflection, respectively. Therefore, $dr_0$ and $dr_1$ can be written as follows

$$d\vec{r}_0 = dx\vec{i} + dy\vec{j} + dz\vec{k} \tag{31}$$

$$d\vec{r}_1 = (1 + u_0' - \xi\theta')\vec{i} + d\eta\vec{j} + (w'dx + d\xi)\vec{k} \tag{32}$$

Considering Eqn. (11) and Eqn. (14), the strain components are derived as follows for a Timoshenko beam

$$\varepsilon_{xx} = u_0' - \xi w'' + \frac{(u_0')^2}{2} + \frac{\xi^2(\theta')^2}{2} - u_0'\theta'\xi + \frac{w'^2}{2} \tag{33}$$

$$\varepsilon_{x\eta} = 0 \tag{34}$$

$$\varepsilon_{x\xi} = (w' - \theta) + \xi\theta\theta' - u_0'\theta \tag{35}$$

In order to obtain simpler expressions for the strain components given by Eqns. (33)-(35), higher order terms can be neglected, so an order of magnitude analysis is performed by using the ordering scheme given by (Ozgumus Ozdemir and Kaya, 2008) and introduced in Table 4.

Table 4. Ordering Scheme for A Timoshenko Beam

| | |
|---|---|
| $\frac{x}{L} = O(1)$ | $\frac{w}{L} = O(\varepsilon)$ |
| $\frac{\eta}{L} = O(\varepsilon)$ | $\frac{\xi}{L} = O(\varepsilon)$ |
| $\frac{u_0}{L} = O(\varepsilon^2)$ | $\theta = O(\varepsilon)$ |
| $\gamma = w' - \theta = O(\varepsilon^2)$ | |

Applying the ordering scheme to Eqns. (33)-(35), the simplified strain components are obtained.

Derivation of The Potential Energy Expression

In the potential energy formulation of a Timoshenko beam, both bending and shear contributions appear in the derivation of the energy expression.

The potential energy contribution due to flapwise bending, $U_b$, is given by

$$U_b = \frac{1}{2}\int_0^L \left( \iint_A E\varepsilon_{xx}{}^2 d\eta d\xi \right) dx \tag{36}$$

The potential energy contribution due to shear, Us, is given by

$$U_s = \frac{1}{2}\int_0^L \left( \iint_A kG\varepsilon_{x\xi}^2 d\eta d\xi \right) dx \tag{37}$$

Here, k is the shear correction factor and G is the shear modulus.

Substituting the related strain components into Eqn.(36) and Eqn.(37), and applying the area integrals of Table 2, the final form of the potential energy is obtained as follows

$$U_T = U_b + U_s = \frac{1}{2}\int_0^{L_e} \left[ EI_y(\theta')^2 + kAG(w' - \theta)^2 + F_{MK}(x)(w')^2 \right] dx + C_1 \tag{38}$$

Derivation of The Kinetic Energy Expression

Considering Eqn.(23), the velocity field components for a rotating Timoshenko beam are obtained. Substituting these expressions into Eqn.(23) and applying the area integrals of Table 3, the kinetic energy expression is derived

$$T = \frac{1}{2}\int_0^{L_e} \left( \rho A \dot{w}^2 + \rho I_y \dot{\theta}^2 + \rho I_y \Omega^2 \theta^2 \right) dx + C_2 \tag{39}$$

Finite Element Formulation

Finite element formulation of a rotating, axially functionally graded beam that undergoes flapwise bending deflection is carried out in this section.

The global finite element model of the beam used for the formulation is illustrated in Fig. 6

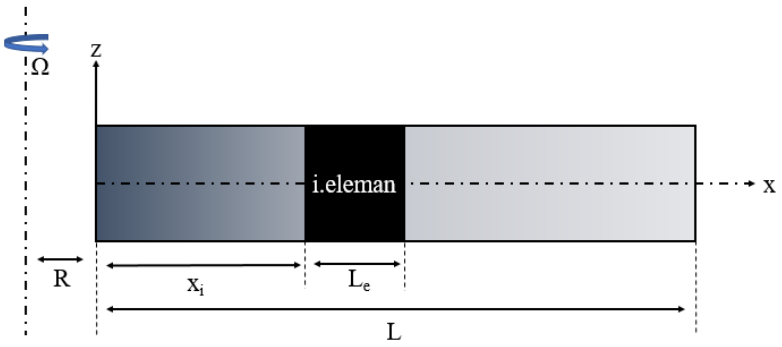


Figure 6. Finite Element Model of A Rotating Axially Functionally Graded Beam

Finite Element Modeling of The Euler Bernoulli Beam

The finite element model of a rotating Euler-Bernoulli beam element is given in Fig. 7.

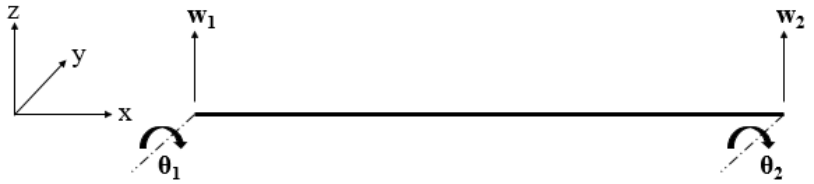


Figure 7: Finite Element Model of The Euler-Bernoulli Beam Element that Undergoes Flapwise Bending

Here, it is seen that a two noded beam element that has four degrees of freedom is preferred to model the beam. Here, w is the flapwise bending and θ is the angle due to flapwise bending.

Polinomials of appropriate order are defined for the displacement field as follows

$$w = a_0 + a_1 x + a_2 x^2 + a_3 x^3 \tag{40}$$

$$\theta = w' = a_1 + 2a_2 x + 3a_3 x^2 \tag{41}$$

Considering the displacement field polinomials given by Eqn. (40) and Eqn.(41), the nodal displacements are determined as the displacement values at the first node of the element, x=0, and at the second node, x=L, respectively. These are given in matrix form as follows

$$\begin{Bmatrix} w_1 \\ \theta_1 \\ w_2 \\ \theta_2 \end{Bmatrix} = \begin{bmatrix} 1 & 0 & 0 & 0 \\ 0 & 1 & 0 & 0 \\ 1 & L_e & L_e^2 & L_e^3 \\ 0 & 1 & 2L_e & 3L_e^2 \end{bmatrix} \begin{Bmatrix} a_0 \\ a_1 \\ a_2 \\ a_3 \end{Bmatrix} \tag{42}$$

Relation between the displacement field and the nodal displacements is

$$\{q\} = [N]\{q_e\} \tag{43}$$

where for the present beam model, expressions of the displacements, {q}, the nodal displacements, $\{q_e\}$ and the matrix of the shape functions, [N] are given

$$\{q\} = \{w \quad \theta\}^T \tag{44}$$

$$\{q_e\} = \{w_1 \quad \theta_1 \quad w_2 \quad \theta_2\}^T \tag{45}$$

$$[N] = [N_w \quad N_\theta]^T \tag{46}$$

Here, $(\,)_1$ are the displacement values of the 1st node while $(\,)_2$ are the displacements on the 2nd node.

Considering the effect of centrifugal force and substituting the shape functions into the potential and kinetic energy expressions, i.e. Eqn. (21) and Eqn.(24), the element stiffness matrice, [$K^e$], and element mass matrice, [$M^e$], are obtained as follows

$$[K^e] = \frac{1}{2}\int_0^{L_e} \left( EI_y \left[\frac{dN_\theta}{dx}\right]^T \left[\frac{dN_\theta}{dx}\right] + F_{MK}(x) \left[\frac{dN_w}{dx}\right]^T \left[\frac{dN_w}{dx}\right] \right) dx \tag{47}$$

$$[M^e] = \frac{1}{2}\int_0^{L_e} \left( \rho A [N_w]^T [N_w] + \rho I_y [N_\theta]^T [N_\theta] \right) dx \tag{48}$$

where $[N_w]$ , $[N_{\theta y}]$ and $[N_\varphi]$ are the shape functions associated with flapwise bending, , rotation due to bending, $\theta_y$ and the shear angle, respectively. The element stiffness matrix is derived from the potential energy expression and the element mass matrice is derived from the kinetic energy expression.

Finite Element Modeling of The Timoshenko Beam

The finite element model of a rotating Timoshenko beam element is given in Fig.8. Here, it is seen that a two noded beam element that has six degrees of freedom is preferred to model the beam. Here, w is the flapwise bending, θ is the angle due to flapwise bending and ϕ is shear angle which is the result of Timoshenko beam formulation.

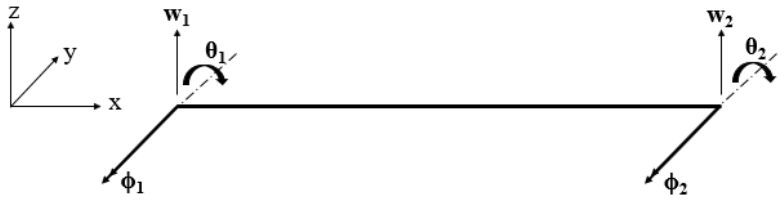


Figure 8: Finite Element Model of the Timoshenko Beam Element that Undergoes Flapwise Bending

Polinomials of appropriate order are defined for the displacement field as follows

$$w = a_0 + a_1 x + a_2 x^2 + a_3 x^3 \tag{49}$$

$$\varphi = a_4 + a_5 x \tag{50}$$

$$\theta = w' - \varphi = a_1 - a_4 + (2a_2 - a_5)x + 3a_3 x^2 \tag{51}$$

Following the steps given by Eqns.(42)-(46), the element stiffness matrice, $[K^e]$, and element mass matrice, $[M^e]$, are obtained as follows

$$\begin{aligned}\left[K^e\right] = \frac{1}{2}\int_0^L \Bigg( EI_y \left[\frac{dN_\theta}{dx}\right]^T \left[\frac{dN_\theta}{dx}\right] + kAG\left(\left[\frac{dN_w}{dx}\right] - N_\theta\right)^T \left(\left[\frac{dN_w}{dx}\right] - N_\theta\right) \\ + F_{MK}(x)\left[\frac{dN_w}{dx}\right]^T \left[\frac{dN_w}{dx}\right]\Bigg) dx\end{aligned} \tag{52}$$

$$\left[M^e\right] = \frac{1}{2}\int_0^L \left(\rho A\left[N_w\right]^T \left[N_w\right] + \rho I_y \left[N_\theta\right]^T \left[N_\theta\right]\right) dx \tag{53}$$

Here $[N_w]$, $[N_\theta]$ and $[N_\varphi]$ are the shape functions associated with the flapwise bending, w, angle due to flapwise bending, θ and shear angle, φ, respectively.

Reduced Global Matrices and Modal Analysis

Depending on the number of elements used in the finite element modeling code, all the element matrices are assembled by considering the finite element rules to obtain the global matrices. The boundary conditions are applied to the global matrices to get the reduced matrices and the following matrix system of equations are obtained

$$[M]\{\ddot{q}\}+[K]\{q\}=\{0\} \tag{54}$$

where [M] and [K] are the reduced global mass and reduced global stiffness matrices, respectively.

Modal analysis is applied to Eqn.(54) to calculate the natural frequencies. Firstly, the modal matrix, [Φ], is calculated by using the eigenvectors obtained by solving the following determinant

$$\det\left[\left[K\right]-\omega^2\left[M\right]\right]=0 \tag{55}$$

Solving Eqn.(82), natural frequencies are calculated for the Euler Bernoulli and Timoshenko beam models.

## RESULTS

In this section, vibration analysis of both Euler-Bernoulli and Timoshenko beams having different boundary conditions and material distribution properties are carried out by using the inhouse computer code that is achieved in MATLAB.

The results are given in several tables and figures which is expected to be a very good source for the researchers who study in the field of axially functionally graded, rotating beams. When the results are compared with the ones in open literature, it is noticed that there is a very good agreement between the results which proves the correctness and accuracy of the studies in this paper.

### Dimensionless Parameters

To be able to make comparisons with the studies in open literature, the following dimensionless parameters given below are defined (Ozdemir O.,2016).

$$\mu=\omega\sqrt{\frac{\rho A_0 L^4}{EI_{y0}}} \tag{56}$$

$$\bar{\Omega}=\Omega\sqrt{\frac{\rho A_0 L^4}{EI_{y0}}} \tag{57}$$

$$r=\sqrt{\frac{I_{y0}}{A_0 L^2}} \tag{58}$$

$$\boldsymbol{\sigma}=\frac{\boldsymbol{R}}{\boldsymbol{L}}$$

Here μ is the dimesionless frequency parameter, $\bar{\boldsymbol{\Omega}}$ is the dimensionless angular speed parameter, r is the inverse of the slenderness ratio parameter and $\boldsymbol{\sigma}$ is the dimensionless hub radius parameter.

### Euler-Bernoulli Beam Results

Vibration characteristics are examined for Euler Bernoulli beam that have axially functionally graded material properties. The beam model used for the analysis is shown in Fig.9

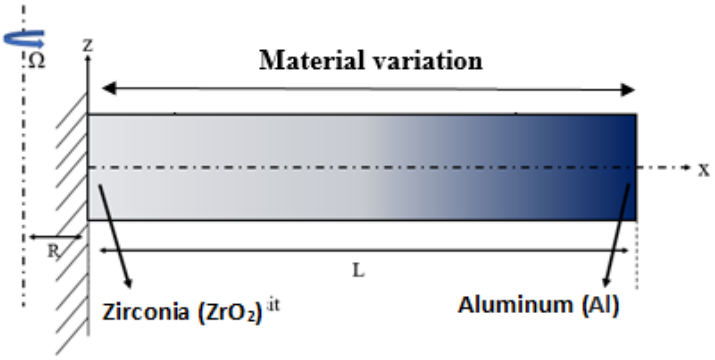


Figure 9: Rotating, Axially Functionally Graded, Cantilevered Beam

The material properties of Aluminum and Zirconia that are used for the AFG Timoshenko beam model are given in Table 5. Here, the beam material is pure $ZrO_2$ at the left end where the beam is fixed and it is pure Al at the right end where the beam is free.

Table 5: Material Properties of the AFG Beam

| Property | Zirconia ($ZrO_2$) | Aluminum (Al) |
|---|---|---|
| **Elasticity Modulus. E** | 200 GPa | 70 GPa |
| **Material Density. ρ** | 5700 kg/m$^3$ | 2702 kg/m$^3$ |
| **Poisson's Ratio υ** | 0.3 | 0.3 |

Vibration characterics of a rotating, functionally graded Euler-Bernoulli beam is examined for two different cases. In the first case, the beam has fixed-free end conditions while in the second case, the beam has fixed-fixed end conditions

Variation of the Modulus of Elasticity, E, along the beam length, i.e. Eqn.(3), with respect to the power law index, n is shown in Fig.10.

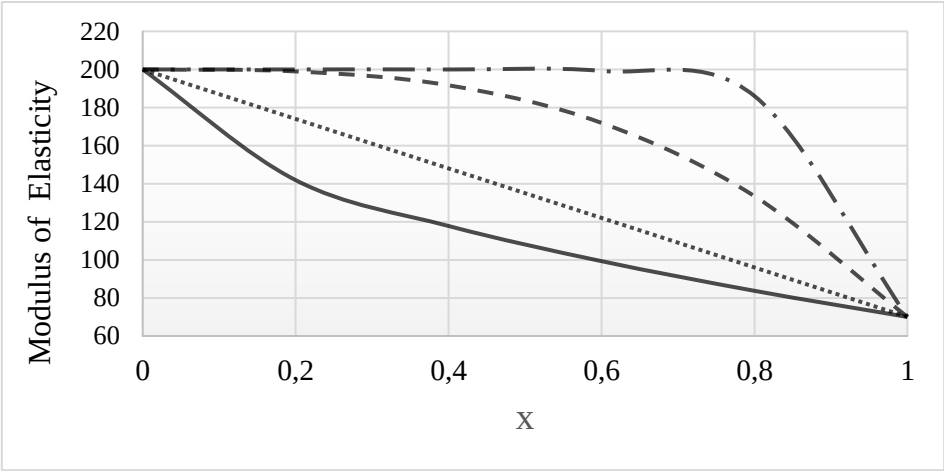


Figure 10: Variation of the Modulus of Elasticity with the Power Law Exponent

Variation of the dimensionless natural frequencies with the functional gradient constant, n, is given in Table 6 and Table 7 for the first and second cases, respectively. As an addition to the material properties given in Table 4, the beam rotates at dimensionless angular speed, Ω=5, the height of the beam is $h_0$=0.0789 m and length of the beam is L=3 m.

Table 6: Dimensionless Natural Frequencies of Axially Functionally Graded Euler Bernoulli Beam with Fixed-Free End Conditions

| Dimensionless Natural Frequencies | | | |
|---|---|---|---|
| **Power Law Exponent (n)** | **Rajasekaran (2013).** | | **Present** |
| | **DQEL** | **DTM** | |
| 1 | 6.9717 | 6.9717 | 7.4656 |
| | 25.6522 | 25.6522 | 26.1552 |
| | 63.3094 | 63.3094 | 63.644 |
| | 119.5321 | 119.5321 | 119.337 |
| 2 | 6.9289 | 6.9289 | 7.5487 |
| | 26.0438 | 26.044 | 26.6992 |
| | 64.6733 | 64.6721 | 65.1456 |
| | 122.1691 | 120.6797 | 122.073 |

Here, in Table 6, the calculated results are compared with open literature where the Differential Quadrature Element Method of Lowest Order (DQEL) and the Differential Transformation Method (DTM) are applied.

Table 7: Dimensionless Natural Frequencies of Axially Functionally Graded Euler Bernoulli Beam with Fixed-Fixed End Conditions

| **Dimensionless Natural Frequencies** | | | |
|---|---|---|---|
| **Power Law Exponent (n)** | **Rajasekaran (2013).** | | **Present** |
| | **DQEL** | **DTM** | |
| 1 | 22.7497 | 22.7497 | 23.1725 |
| | 60.6397 | 60.6397 | 61.0181 |
| | 116.956 | 116.956 | 116.946 |
| | 191.8536 | 191.8519 | 191.044 |
| 2 | 22.3542 | 22.3542 | 22.7186 |
| | 60.6611 | 60.6611 | 61.0345 |
| | 117.9543 | 117.9543 | 117.979 |
| | 194.2642 | 194.259 | 193.54 |

Timoshenko Beam Results

In this section, vibration characterics of a functionally graded Timoshenko beam is examined for two different cases. In the first case, the beam has fixed-free end conditions while in the second case, the beam has fixed-fixed end conditions

Variation of the dimensionless natural frequencies with the functional gradient constant, n, is given in Table 8 and Table 9 for the first and second cases, respectively. As an addition to the material properties given in Table 5, the slenderness ratio is $r = 0.01\ m$, length of the beam is L= $5\ m$ and the shear correction factor is k=5/6.

Table 8: Dimensionless Natural Frequencies of Axially Fuctionally Graded Timoshenko Beam with Fixed-Free End Conditions

| Dimensionless Natural Frequencies (Fixed-free) | | | | | |
|---|---|---|---|---|---|
| **Power Law Exponent (n)** | **Shahba et al., 2011** | **Present** | **Functional gradient constant (n)** | **Shahba et al., 2011** | **Present** |
| 0.3 | 3.5 | 3.5222 | 1.8 | 3.93 | 3.9576 |
| | 14.25 | 14.3333 | | 15.2 | 15.4732 |
| | 29.7 | 30.0593 | | 31.6 | 32.0377 |
| | 44.5 | 45.0699 | | 48 | 48.203 |
| 0.6 | 3.79 | 3.7580 | 2.1 | 3.92 | 3.9458 |
| | 14.75 | 14.8256 | | 15.25 | 15.5248 |
| | 30.4 | 30.7528 | | 31.7 | 32.2145 |
| | 45.8 | 46.0706 | | 48.2 | 48.5221 |
| 0.9 | 3.9 | 3.8815 | 2.4 | 3.9 | 3.9283 |
| | 15 | 15.1141 | | 15.3 | 15.562 |
| | 30.9 | 31.2279 | | 31.8 | 32.367 |
| | 46 | 46.8072 | | 48.3 | 48.7959 |
| 1.2 | 3.95 | 3.9388 | 2.7 | 3.85 | 3.9083 |
| | 15.1 | 15.2884 | | 15.3 | 15.5894 |
| | 31.2 | 31.5676 | | 32 | 32.5002 |
| | 47 | 47.3725 | | 48.4 | 49.0328 |
| 1.5 | 3.94 | 3.9585 | 3.0 | 3.8 | 3.9068 |
| | 15.15 | 15.3991 | | 15.3 | 15.2337 |
| | 31.58 | 31.8274 | | 32.2 | 31.5458 |
| | 47.7 | 47.8264 | | 48.5 | 47.3647 |

Table 9: Dimensionless Natural Frequencies of Axially Fuctionally Graded Timoshenko Beam with Fixed-Fixed End Conditions

| Dimensionless Natural Frequencies (Fixed-fixed) | | | | | |
|---|---|---|---|---|---|
| **Power Law Exponent (n)** | **Shahba et al., 2011** | **Present** | **Functional gradient constant (n)** | **Shahba et al., 2011** | **Present** |
| 0.3 | 12.87 | 13.0648 | 1.8 | 12.62 | 12.9043 |
| | 26.78 | 27.0523 | | 26.64 | 27.4202 |
| | 43.3 | 43.2826 | | 43.6 | 44.7496 |
| | 59 | 57.8758 | | 59.72 | 60.4913 |
| 0.6 | 12.79 | 13.1393 | 2.1 | 12.6 | 12.8521 |
| | 26.74 | 27.3592 | | 26.63 | 27.3899 |
| | 43.4 | 43.9353 | | 43.62 | 44.8206 |
| | 59.3 | 58.9581 | | 59.74 | 60.6404 |
| 0.9 | 12.73 | 13.1071 | 2.4 | 12.595 | 12.8107 |
| | 26.7 | 27.4601 | | 26.62 | 27.3639 |
| | 43.49 | 44.2982 | | 43.64 | 44.8741 |
| | 59.5 | 59.5987 | | 59.78 | 60.7522 |
| 1.2 | 12.68 | 13.0393 | 2.7 | 12.592 | 12.779 |
| | 26.67 | 27.4724 | | 26.61 | 27.3432 |
| | 43.55 | 44.5135 | | 43.7 | 44.915 |
| | 59.62 | 60.0089 | | 59.8 | 60.8359 |

Variation of the fundamental natural frequencies of a rotating axially functionally graded Timoshenko beam with respect to the rotational speed parameter, $\bar{\Omega}$ and the hub radius parameter,σ is demonstrated in Figs.11 for n=1. Here, the dotted line gives the frequency values calculated for σ = 0, the dashed line is for σ = 0.2 and the solid line is for σ = 0.4.

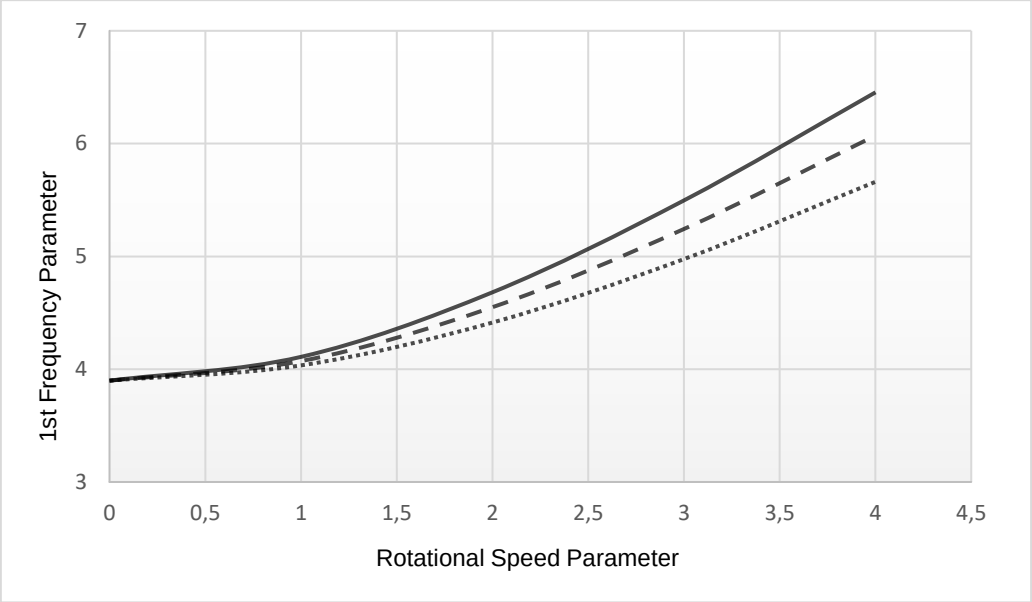


## References

Alshorbagy AE. Eltaher MA and Mahmoud FF (2011). Free Vibration Characteristics of A Functionally Graded Beam by Finite Element Method. Applied Mathematical Modelling. 35: 412–425.

Bhimaraddi A. and Chandrashekhara K. (1991). Some Observation on The Modeling of Laminated Composite Beams with General Lay-Ups. Composite Structures. 19: 371–380.

Chakraborty A. Gopalakrishnan S and Reddy JN (2003). A New Beam Finite Element for The Analysis of Functionally Graded Materials. International Journal of Mechanical Sciences. 45: 519–539.

Eringen, A. C. (1980). Mechanics of continua. Huntington, NY, Robert E. Krieger Publishing Co., 1980. 606 p.

Giunta G. Crisafulli D. Belouettar S and Carrera E. (2011). Hierarchical Theories for The Free Vibration Analysis of Functionally Graded Beams. Composite Structures. 94: 68–74.

Hodges, D. H., & Dowell, E. H. (1974). Nonlinear equations of motion for the elastic bending and torsion of twisted nonuniform rotor blades.

Huang Y and Li XF. (2010). A New Approach for Free Vibration of Axially Functionally Graded Beams with Non-Uniform Cross-Section. Journal of Sound and Vibration. 329: 2291–2303.

Kapuria S. Bhattacharyya M and Kumar AN. (2008). Bending and Free Vibration Response of Layered Functionally Graded Beams: A Theoretical Model and Its Experimental Validation. Composite Structures. 82: 390–402.

Lai SK. Harrington J. Xiang Y and Chow KW. (2012). Accurate Analytical Perturbation Approach for Large Amplitude Vibration of Functionally Graded Beams. International Journal of Non-Linear Mechanics. 47: 473–480.

Li XF. (2008). A Unified Approach for Analyzing Static and Dynamic Behaviors of Functionally Graded Timoshenko and Euler–Bernoulli Beams. Journal of Sound and Vibration. 318: 1210–1229.

Loja MAR. Barbosa JI and Mota Soares CM. (2012). A Study on The Modelling of Sandwich Functionally Graded Particulate Composite. Composite Structures. 94: 2209–2217.

Loy CT. Lam KY and Reddy JN (1999). Vibration of Functionally Graded Cylinderical Shells. International Journal of Mechanical Science. 41: 309-324.

Lu CF and Chen WQ. (2005). Free Vibration of Orthotropic Functionally Graded Beams with Various End Conditions. Structural Engineering and Mechanics. 20: 465–476.

Ozdemir O. (2016) Application of The Differential Transform Method to the Free Vibration Analysis of Functionally Graded Timoshenko Beams, Journal of Theoretical And Applied Mechanics, 54, 4, 1205-1217.
Ozdemir O. (2019) Vibration Analysis Of Rotating Timoshenko Beams with Different Material Distribution Properties. Selçuk University, Journal of Science, Engineering and Technology, vol. 7(2), pp. 272-286.

Ozgumus Ozdemir O. (2012). Dynamic and Aeroelastic Analysis of A Helicopter Blade with An Actively Controlled Trailing Edge Flap in Forward Flight, Ph.D Thesis, Istanbul Technical University, Istanbul.

Ozgumus Ozdemir O. and Kaya, M. O. (2008). Flapwise bending vibration analysis of a rotating double-tapered Timoshenko beam. Archive of Applied Mechanics, 78(5), 379-392.

Thai HT and Vo TP. (2012). Bending and Free Vibration of Functionally Graded Beams Using Various Higher-Order Shear Deformation Beam Theories. International Journal of Mechanical Sciences. 62: 57–66.

Rajasekaran, S. (2013). Differential transformation and differential quadrature methods for centrifugally stiffened axially functionally graded tapered beams. International Journal of Mechanical Sciences, 74, 15-31.

Shahba, A., Attarnejad, R., Marvi, M. T., & Hajilar, S. (2011). Free vibration and stability analysis of axially functionally graded tapered Timoshenko beams with classical and non-classical boundary conditions. Composites Part B: Engineering, 42(4), 801-808.

Wattanasakulpong N. Prusty BG. Kelly DW and Hoffman M. (2012). Free Vibration Analysis of Layered Functionally Graded Beams with Experimental Validation. Materials & Design. 36: 182–190.

Yang, J. B., Jiang, L. J., & Chen, D. C. (2004). Dynamic modelling and control of a rotating Euler–Bernoulli beam. Journal of sound and vibration, 274(3-5), 863-875.

Zhong Z. and Yu T. (2007). Analytical Solution of A Cantilever Functionally Graded Beam. Composites Science and Technology. 67: 481–488.